Infrared stability of de Sitter QFT: Results at all orders

Donald Marolf and Ian A. Morrison

Phys. Rev. D **84**, 044040 — Published 16 August 2011

DOI: 10.1103/PhysRevD.84.044040

The IR stability of de Sitter QFT: results at all orders

Donald Marolf* and Ian A. Morrison†
University of California at Santa Barbara, Santa Barbara, CA 93106, USA

We show that the Hartle-Hawking vacuum for any theory of interacting massive scalars on a fixed de Sitter background is both perturbatively well-defined and stable in the IR. Correlation functions in this state may be computed on the Euclidean section and Wick-rotated to Lorentz-signature. The results are manifestly de Sitter-invariant and contain only the familiar UV singularities. More importantly, the connected parts of all Lorentz-signature correlators decay at large separations of their arguments. Our results apply to all cases in which the free Euclidean vacuum is well defined, including scalars with masses belonging to both the complementary and principal series of $SO(D,1)$. This suggests that interacting QFTs in de Sitter – including higher spin fields – are perturbatively IR-stable at least when i) the Euclidean vacuum of the zero-coupling theory exists and ii) corresponding Lorentz-signature zero-coupling correlators decay at large separations. This work has significant overlap with a paper by Stefan Hollands, which is being released simultaneously.

Keywords: de Sitter, Infra-red divergences, QFT in curved spacetime, interacting QFT

* marolf@physics.ucsb.edu
† ian_morrison@physics.ucsb.edu

I. INTRODUCTION

While free quantum fields in de Sitter space (dS_D) have been well understood for some time (see [1] for scalar fields), interacting de Sitter quantum field theory continues to be a topic of much discussion. In particular, there has been significant interest in the possibility of large infrared (IR) effects in interacting de Sitter quantum field theories [2–26], both with and without dynamical gravity.

In [27] we began to address the specific class of such concerns associated with infra-red (IR) divergences of the naive Lorentz-signature de Sitter Feynman diagrams, or more generally those concerns that can be addressed in the context of minimally-coupled scalar fields with mass $M^2 > 0$ on a fixed de Sitter background; i.e., in a context where gravity is non-dynamical. There we computed one-loop corrections to propagators on Euclidean de Sitter (which is just the D-sphere S^D) and analytically continued the results to Lorentz-signature. This procedure defines the so-called Hartle-Hawking vacuum of the Lorentzian theory [28], which on general grounds should be a good quantum state (see section V). In particular, the analytically continued correlators are expectation values of products of operators in a single state as opposed to matrix elements between an "in-vacuum" and a potentially different "out-vacuum." We do not attempt to define any notion of S-matrix.

Because S^D is compact, it is a priori clear that Euclidean correlators do not suffer infra-red divergences. We showed in [27] that, to one-loop order, the analytically continued Lorentz-signature correlators were also finite and decayed at a rate determined by the lightest relevant mass[1]. The purpose of the current paper is to extend these results to arbitrary N-point functions and to all orders in perturbation theory, again showing that connected correlators decay rapidly as the separation between points becomes large. As in [27], our results will apply to all masses for which the free Euclidean de Sitter vacuum is well-defined, i.e. for all $M^2 > 0$, including values in both the complimentary series and the principal series of $SO(D, 1)$. We again emphasize that we consider massive scalar quantum field theories on a fixed de Sitter background, taking gravity to be non-dynamical. Due to the growth of the graviton propagator at large distances, introducing a dynamical graviton could lead to radically different results than those reported below.

Nevertheless, we also emphasize that the decay of connected correlators found below demonstrates that the Hartle-Hawking vacuum of any massive scalar field theory is perturbatively stable, and that the Hartle-Hawking vacuum is an attractor state for local operators in the sense defined in [27]. To explain this point in detail, let us consider a state constructed from the Hartle-Hawking vacuum $|0\rangle_{HH}$ with appropriately smeared operators:

$$|\Psi\rangle := \int_{Y_1} \dots \int_{Y_n} f(Y_1, \dots, Y_n) \phi_\sigma(Y_1) \cdots \phi_\sigma(Y_n) |0\rangle_{HH}. \tag{1}$$

Here the Y_i are points in dS_D, $\int_Y \dots$ denotes an integral over de Sitter, and $f(Y_1, \dots, Y_n)$ is a smearing function which we assume to be supported in a compact domain $\mathcal{D}$. Now examine the correlation function $\langle \Psi | \phi_\sigma(X_1) \cdots \phi_\sigma(X_N) | \Psi \rangle$ with all X_i at large separations from $\mathcal{D}$. In this configuration the correlator is simply a smeared correlation function between $2n$ operators located within $\mathcal{D}$ and N operators with large (say, roughly equal) separations $|Z|$ from $\mathcal{D}$ evaluated in the Hartle-Hawking vacuum. Since the associated connected correlators decay rapidly at large separations, this function approximately factorizes into a product of two correlators: one for the points in $\mathcal{D}$ and one for the other points. The former factor is just the norm of $|\Psi\rangle$, so we have $\langle \Psi | \phi_\sigma(X_1) \cdots \phi_\sigma(X_N) | \Psi \rangle \rightarrow \langle \Psi | \Psi \rangle \cdot {}_{HH}\langle 0 | \phi_\sigma(X_1) \cdots \phi_\sigma(X_N) | 0 \rangle_{HH}$. This means that, as probed by local operators, the excited state $|\Psi\rangle$ becomes indistinguishable from the Hartle-Hawking vacuum. Thus, despite concerns raised in [30–33] associated with the lack of a conserved positive definite energy and other issues in de Sitter space, our results below provide a very physical sense in which the Hartle-Hawking vacuum of any massive scalar field theory is stable. Note that, although the above argument was phrased in terms of the elementary field ϕ_σ, the fact that composite operators can be defined by the operator product expansion with respect to geodesic distance [34] implies that the same conclusion immediately follows for all composite local operators built from such fundamental fields.

We begin by briefly reviewing free de Sitter quantum field theory in section II. We then address simple tree diagrams in section III, which also serves to introduce some useful Mellin-Barnes techniques and our choice of (Pauli-Villars) regularization scheme. We address general diagrams in section IV, where we establish the desired results for finite Pauli-Villars regulator masses (so that all diagrams are finite). Since the infra-red asymptotics are independent of the regulator masses, it is straightforward to take the limit where such regulators are removed[2]. Some technical material is relegated to the appendices. We close with some discussion in section V.

Remark: While paper was being prepared, we received a draft of [36] which reports similar results.

---

[1] In addition, the one-loop calculations reported in [29] establish that correlators of free-field stress tensors decay at large separations.

[2] After subtracting regulator-dependent local counter-terms in order to obtain a finite result. We consider theories can be renormalized in this way. One would expect this procedure to be equivalent (up to finite local counter-terms) to the renormalization prescription given in [35], and thus to define a fully covariant renormalized quantum field theory in the sense of [34] whenever the flat-space limit is power-counting renormalizable. However, we have not analyzed this question in detail and save any investigation for future work.

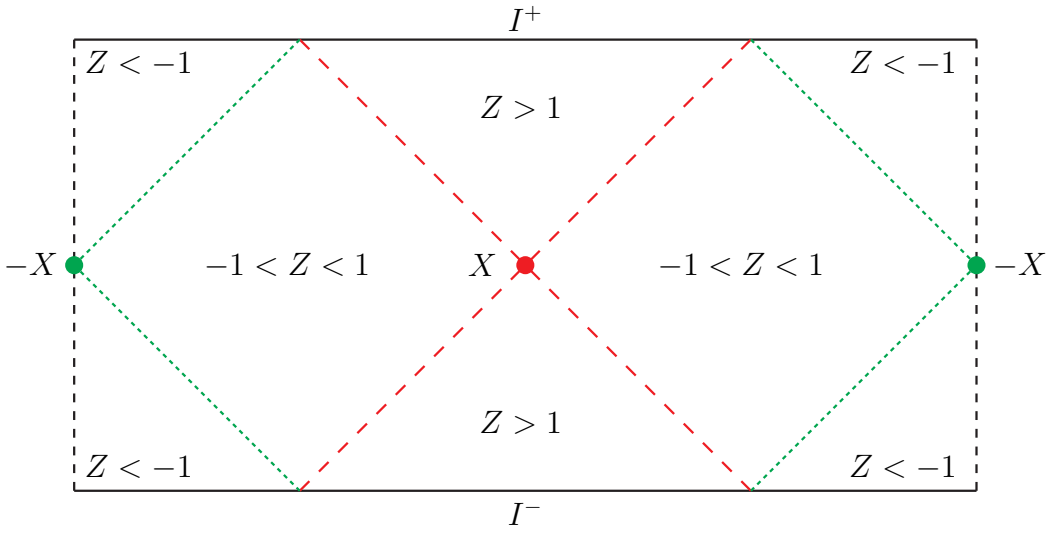

FIG. 1. The conformal diagram of global de Sitter. The dashed ends are identified. Shown are the points X and the corresponding antipodal point $-X$. Values of the embedding distance $Z := XY/\ell^2$ in different regions of de Sitter are labeled; in addition, the dashed red lines denote the lightcone with $Z = 1$ and the dotted green lines denote the lightcone with $Z = -1$ [1].

II. FREE DE SITTER QFT

This brief section serves as a review of scalar quantum field theory in de Sitter and allows us to establish our notation. We consider D-dimensional de Sitter space dS_D with radius ℓ, which may be defined as the single-sheet hyperboloid in a $D+1$-dimensional Minkowski space M_{D+1}. Points on de Sitter satisfy [37]

$$\eta_{AB} X^A X^B = \ell^2, \tag{2}$$

where X^A is a vector in the embedding space and $\eta_{AB} = \text{diag}(-1, 1, \ldots, 1)$ is the usual Minkowski metric. Henceforth we will drop the index notation and denote the inner product of two embedding space vectors X_1 and X_2 simply by $X_1 \cdot X_2$. For two points on de Sitter located at X_1 and X_2 the inner product $X_1 \cdot X_2/\ell^2$ provides a convenient measure of distance which we loosely call the *embedding distance* between X_1 and X_2 [1]. The embedding distance is related to the length of the chord between X_1 and X_2 in the embedding space (with the length being proportional to $1 - X_1 \cdot X_2$) and is clearly invariant under the full de Sitter isometry group $SO(D, 1)$. The embedding distance satisfies:

- $X_1 \cdot X_2/\ell^2 \in [-1, 1)$ for spacelike separation,
- $X_1 \cdot X_2/\ell^2 = 1$ for null separation, and
- $|X_1 \cdot X_2/\ell^2| > 1$ for timelike separation.

The antipodal point of X_1 is simply $-X_1$; clearly the embedding distance between antipodal points is -1. See Figure 1.

In this work we restrict attention to massive scalar fields $\phi_\sigma(X)$. It is convenient to keep track of the spacetime dimension with the parameter $\alpha = (D-1)/2$; the mass parameter σ is then defined by the equation

$$-\sigma(\sigma + 2\alpha) = M^2\ell^2, \tag{3}$$

where M^2 is the bare mass-squared of the field if we assume minimal coupling to the metric. There is a redundancy in this definition as (3) is invariant under $\sigma \to -(\sigma + 2\alpha)$; for clarity we choose to define σ as the positive root

$$\sigma := -\alpha + \left(\alpha^2 - M^2\ell^2\right)^{1/2}, \tag{4}$$

but all expressions involving σ must necessarily be invariant under $\sigma \to -(\sigma + 2\alpha)$. Free scalar fields form irreducible representations of the de Sitter group $SO_0(D, 1)$ and fall into three series [38]:

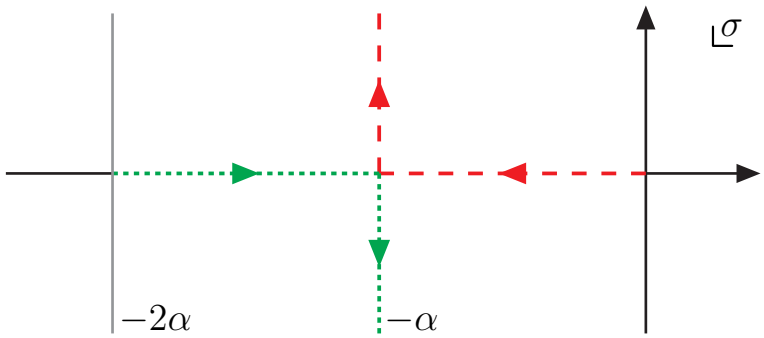

FIG. 2. On-shell values of σ and $-(\sigma+2\alpha)$ in the complex plane for massive scalar fields. The red dashed line denotes the path of σ for increasing M^2 starting from at $\sigma = 0$ for $M^2 = 0$. The green doted line shows the path of $-(\sigma+2\alpha)$ for increasing M^2 starting from $-(\sigma+2\alpha) = -2\alpha$ for $M^2 = 0$. Relatively light fields with $0 < M^2\ell^2 < \alpha^2$ correspond to values of σ and $-(\sigma+2\alpha)$ on the negative real axis and belong to the complementary series. Heavier fields with $M^2\ell^2 \geq \alpha^2$ correspond to complex values of σ and $-(\sigma+2\alpha)$ on the line defined by $\mathrm{Re}\,\sigma = \mathrm{Re}\,(-\sigma-2\alpha) = -\alpha$.

1. complementary series: $-\alpha < \sigma < 0$,
2. principal series: $\sigma = -\alpha + i\rho,\ \rho \in \mathbb{R},\ \rho \geq 0$,
3. discrete series: $\sigma = 0, 1, 2, \ldots$.

We plot σ and $-(\sigma+2\alpha)$ as a function of $M^2 > 0$ in figure 2. Relatively light massive fields belong to the complimentary series while heavier fields belong to the principal series. It is useful to note that $\sigma_{cc} = \frac{1}{2} - \alpha$ corresponds to an otherwise massless conformally coupled free field. This value lies in the complimentary series so long as $D > 2$. Discrete series fields correspond to massless and tachyonic scalars and we will not consider them here.

Free massive scalar fields admit a unique de Sitter-invariant Hadamard vacuum $|0\rangle_{\rm free}$, commonly referred to as the Euclidean vacuum (it is also the Bunch-Davies vacuum) [1, 3]. Since the theory is free, the vacuum is completely characterized by its 2-point functions. Let us define the function

$$\Delta_\sigma(Z) := \frac{\ell^{2-D}}{(4\pi)^{\alpha+1/2}} \frac{\Gamma(-\sigma)\,\Gamma(\sigma+2\alpha)}{\Gamma\left(\frac{1}{2}+\alpha\right)}\, {}_2F_1\left[-\sigma\,,\,\sigma+2\alpha\,;\,\frac{1}{2}+\alpha\,;\,\frac{1+Z}{2}\right]. \tag{5}$$

Here ${}_2F_1(a,b;c;z)$ is the Gauss hypergeometric function. In general this function has a branch point at $Z = 1$ and is cut along the positive real axis $Z \in [1, +\infty)$. The time-ordered and Wightman correlation functions of a massive scalar field $\phi_\sigma(X)$ are given by

$$\langle 0|T\phi_\sigma(X_1)\phi_\sigma(X_2)|0\rangle_{\rm free} = \Delta_\sigma(X_1\cdot X_2 - i\epsilon), \tag{6}$$

$$\langle 0|\phi_\sigma(X_1)\phi_\sigma(X_2)|0\rangle_{\rm free} = \Delta_\sigma(X_1\cdot X_2 - i\epsilon s(X_1,X_2)), \tag{7}$$

where in (7) the operator ordering is enforced by $s(X_1, X_2) = +(-)$ if X_1 is in the future (past) of X_2 (see, e.g., [39]).

At the level of free fields, one may in fact use any member of the one-parameter family of 2-point functions found in [1, 3] to define a de Sitter-invariant vacuum state. These other vacua are usually called Mottola-Allen (MA) or α vacua. However, the non-trivial MA vacua do not satisfy the Hadamard or Bunch-Davies criteria; in particular, their 2-point functions i) have an additional singularity at antipodal points and ii) have an additional negative frequency contribution to the singularity at coincident points [40]. As a result, only the Euclidean vacuum extrapolates to the usual Minkowski vacuum in the flat space limit [41]. It has been difficult to find consistent extensions of MA vacua to interacting theories – see e.g. [39, 42–46]. For these reasons we will discuss only the Euclidean vacuum in this work.

III. SIMPLE TREE DIAGRAMS

We now proceed to analyze simple connected tree diagrams. As noted in the introduction, we compute diagrams on Euclidean S^D and analytically continue the results to de Sitter. In particular, the Mellin-Barnes techniques used below

provide representations of connected diagrams $\mathcal{V}_N(X_1,\ldots,X_n,X_N)$ on S^D in terms of the $N(N-1)/2$ embedding distances $Z_{ij}=X_i\cdot X_j$ relating the external points. While the Z_{ij} are not all independent for general N,D, it will often be convenient to use our Mellin-Barnes representation to extend the definition of $\mathcal{V}_N$ to a function of $N(N-1)/2$ independent variables Z_{ij}. The analytic continuation can then be performed by analytically continuing in each Z_{ij} and evaluating $Z_{ij}=X_i\cdot X_j$ for N points X_i in Lorentz-signature de Sitter space.

The only subtlety in the analytic continuations will be the presence of branch cuts. As noted in section II, for the two-point function this amounts to choosing the appropriate $i\epsilon$ prescription to construct time-ordered or Wightman correlators, as desired. Much the same is true of higher N-point correlators, though the specifics are more complicated to state. However, since our only goal is to extract the asymptotics at large Z_{ij}, we need not be concerned with such details here. The large Z asymptotics are identical on both sides of each cut so that all analytic continuations satisfy the fall-off properties derived below. This means in particular that our results hold for both Wightman and time-ordered correlators.

A. The Green's function

It is convenient for our analysis to use a Mellin-Barnes integral representation of the scalar Green's function on S^D. Mellin-Barnes representations have proved to be quite useful in evaluating Feynman diagrams in flat-space QFT (see, e.g., [47] for an introduction). They are especially convenient for deriving asymptotic expansions (see §4.8 of [47]), and it is for this reason that we choose to use them here. We review some essential information about Mellin-Barnes integrals in Appendix A; further details can be found an any standard text on mathematical methods.

Starting with the case $\sigma<\sigma_{cc}=\frac{1}{2}-\alpha$ and $\alpha\geq\frac{1}{2}$, we may write the scalar Green's function

$$\Delta_\sigma(Z)=\frac{1}{(4\pi)^{\alpha+1/2}\Gamma\left[\frac{1}{2}+\alpha+\sigma,\frac{1}{2}-\alpha-\sigma\right]}\int_\nu\Gamma\left[-\sigma+\nu,\sigma+2\alpha+\nu,-\nu,\frac{1}{2}-\alpha-\nu\right]\left(\frac{1-Z}{2}\right)^\nu, \tag{8}$$

where we use a condensed notation for products and ratios of Γ-functions:

$$\Gamma\left[\begin{array}{c}a_1,\,a_2,\,\ldots,\,a_j\\ b_1,\,b_2,\,\ldots,\,b_k\end{array}\right]:=\frac{\Gamma(a_1)\,\Gamma(a_2)\cdots\Gamma(a_j)}{\Gamma(b_1)\,\Gamma(b_2)\cdots\Gamma(b_k)}, \tag{9}$$

or merely $\Gamma[a_1,\,a_2,\,\ldots,\,a_j]$ for just a product. In (8) the symbol $\int_\nu\ldots$ denotes a contour integral in the complex ν plane. We take as implicit the measure $d\nu/2\pi i$. The contour of integration is a straight line parallel to the imaginary axis traversed from $-i\infty$ to $+i\infty$ anywhere within a region called the "fundamental strip" (FS). In general we denote a fundamental strip by its left and right boundaries $<l,r>$. For the Green's function (8) the fundamental strip is $<\sigma,\frac{1}{2}-\alpha>$ which is non-empty due to the restriction $\sigma<\frac{1}{2}-\alpha$. The integrand is analytic in ν within the FS; beyond the FS it has an infinite number of poles due the Gamma functions. By convention we call poles generated by Gamma functions $\Gamma(\cdots+\nu)$ left poles; likewise, we call poles generated by Gamma functions $\Gamma(\cdots-\nu)$ right poles. The fundamental strip is the region between the left and right poles. For this reason we do not generally need to write the FS explicitly as it may be inferred from the Gamma functions of the integrand.

The asymptotic behavior of $\Delta_\sigma(Z)$ at large $|Z|\gg1$ may be determined by moving the contour to the left. The first of the two series of left poles give the leading asymptotic terms:

$$\begin{aligned}\Delta_\sigma(|Z|>1)=&\frac{1}{4\pi^{\alpha+1}}\left\{\Gamma[-\sigma,\sigma+\alpha](-2Z)^\sigma+\Gamma[\sigma+2\alpha,-\sigma-\alpha](-2Z)^{-\sigma-2\alpha}\right\}\\&\times\left[1+O\left(Z^{-2}\right)\right].\end{aligned} \tag{10}$$

The asymptotic behavior for $|Z|$ near 1 is determined by moving the contour to the right. When D is odd, α is an integer greater than or equal to 1 and the leading behavior is given by

$$\begin{aligned}\Delta_\sigma(|Z|<1)=&\frac{1}{(4\pi)^{\alpha+1/2}}\left\{\Gamma\left(\alpha-\frac{1}{2}\right)\left(\frac{1-Z}{2}\right)^{1/2-\alpha}+\Gamma\left[\begin{array}{c}\frac{1}{2}-\alpha,-\sigma,\sigma+2\alpha\\ \frac{1}{2}-\alpha-\sigma,\frac{1}{2}+\alpha+\sigma\end{array}\right]\right\}\\&\times[1+O(1-Z)].\end{aligned} \tag{11}$$

When D is even $\alpha=\frac{1}{2}+n$, $n\in\mathbb{N}_0$ (where $\mathbb{N}_0$ are the non-negative integers) and the two sets of poles overlap at $\nu\in\mathbb{N}_0$ yielding double-poles. As a result the pole at $\nu=0$ gives a term with logarithmic behavior:

$$\begin{aligned}\Delta_\sigma(|Z|<1)=&\frac{\Gamma(n)}{(4\pi)^{n+1}}\left(\frac{1-Z}{2}\right)^{-n}[1+O(1-Z)]\\&-\frac{1}{(4\pi)^{n+1}}\Gamma\left[\begin{array}{c}1+\sigma+2n\\ 1+\sigma,1+n\end{array}\right]\log(1-Z)+O(1)\end{aligned} \tag{12}$$

(the first term is omitted when $n = 0$).

When $\sigma > \sigma_{cc}$ the left-most right pole in (8) lies to the left of the right-most left pole so that there are can be no straight contour in between. To arrive at an expression valid for all masses, consider again the case $\sigma < \sigma_{cc}$ and move the contour in (8) to the right past the first right pole at $\nu = \frac{1}{2} - \alpha$ to obtain the expression

$$\Delta_\sigma(Z) = \frac{-1}{(4\pi)^{\alpha+1/2}} \int_\nu \Gamma \left[\begin{matrix} -\sigma+\nu, \sigma+2\alpha, -\nu, \frac{3}{2}-\alpha-\nu \\ \frac{1}{2}+\alpha+\sigma, \frac{1}{2}-\alpha-\sigma \end{matrix} \right] \frac{1}{(\nu - \frac{1}{2} + \alpha)} \left(\frac{1-Z}{2}\right)^\nu + \frac{\Gamma\left(\alpha - \frac{1}{2}\right)}{(4\pi)^{\alpha+1/2}} \left(\frac{1-Z}{2}\right)^{1/2-\alpha}. \tag{13}$$

In the integral in the first line the contour lies in the interval $(\max\{\sigma, \frac{1}{2}-\alpha\}, \min\{0, \frac{3}{2}-\alpha\})$. This interval is non-trivial for $\sigma < \frac{3}{2} - \alpha$ (since $\sigma < 0$), and (13) is a valid representation of the propagator for any such σ. This process can be repeated as needed so that one can then increase σ as far into the complementary series as desired. The asymptotic properties when $\sigma > \frac{1}{2} - \alpha$ are again given by (10)-(12). At conformal coupling $\sigma = \frac{1}{2} - \alpha$, only the residue term in (13) survives:

$$\Delta_{\rm cc}(Z) = \frac{\Gamma\left(\alpha - \frac{1}{2}\right)}{(4\pi)^{\alpha+1/2}} \left(\frac{1-Z}{2}\right)^{1/2-\alpha}. \tag{14}$$

The behavior of the Green's function at large $M^2 \gg 1$ will be important to our analysis. Starting with (8) we define

$$\psi_\sigma(\nu) := \frac{1}{(4\pi)^{\alpha+1/2}} \Gamma \left[\begin{matrix} -\sigma+\nu, \sigma+2\alpha+\nu, \frac{1}{2}-\alpha-\nu \\ \frac{1}{2}+\alpha+\sigma, \frac{1}{2}-\alpha-\sigma \end{matrix} \right], \tag{15}$$

so that the Green's function may be written

$$\Delta_\sigma(Z) = \int_\nu \psi_\sigma(\nu) \Gamma(-\nu) \left(\frac{1-Z}{2}\right)^\nu. \tag{16}$$

At large $M^2 \gg 1$ the function $\psi_\sigma(\nu)$ has the asymptotic behavior

$$\psi_\sigma(\nu) = \frac{M^{2\alpha-1+2\nu}}{(4\pi)^{\alpha+1/2}} \Gamma\left(\frac{1}{2} - \alpha - \nu\right) \left(1 + O\left(M^{-2}\right)\right), \tag{17}$$

and as a result the Green's function has the asymptotic behavior

$$\Delta_\sigma(Z) = \frac{M^{2\alpha-1}}{(4\pi)^{\alpha+1/2}} \int_\nu \Gamma\left[-\nu, \frac{1}{2} - \alpha - \nu\right] M^{2\nu} \left(\frac{1-Z}{2}\right)^\nu \left(1 + O\left(M^{-2}\right)\right). \tag{18}$$

Note that (18) contains no left poles; the left poles of the original expression (15) do not appear at any finite order in the expansion in inverse powers of M^2. In the limit $M^2 \to \infty$ the inequality $|M^2(1-Z)/2| > 1$ holds for any fixed $Z \neq 1$, and in this limit the contour in (18) may be closed in the left half-plane giving $\Delta_\sigma(Z \neq 1) = O(M^{-4})$. By examining the action of (18) integrated against a test function (represented as an MB integral) one may determine that (18) is equivalent to

$$\Delta_\sigma(Z) = \frac{1}{M^2} \frac{1}{\text{vol}(S^{2\alpha})} \frac{\delta(Z-1)}{(1-Z^2)^{\alpha-1/2}} + O\left(M^{-4}\right); \tag{19}$$

the first few sub-leading terms are

$$\Delta_\sigma(Z) = \frac{1}{M^2} \frac{1}{\text{vol}(S^{2\alpha})} \frac{\delta(Z-1)}{(1-Z^2)^{\alpha-1/2}} + \frac{1}{M^4} \frac{1}{\text{vol}(S^{2\alpha})} \frac{\partial}{\partial Z} \left[\frac{\delta(Z-1)}{(1-Z^2)^{\alpha-1/2}}\right] + \frac{1}{M^6} \frac{1}{\text{vol}(S^{2\alpha})} \frac{\partial^2}{\partial Z^2} \left[\frac{\delta(Z-1)}{(1-Z^2)^{\alpha-1/2}}\right] + O\left(M^{-8}\right). \tag{20}$$

Of course, the expansion (20) follows from the fact that the Green's function is the inverse of the Klein-Gordon operator using $\frac{\mathbb{1}}{\nabla^2 - M^2} = -M^{-2} \frac{\mathbb{1}}{1 - \nabla^2/M^2} = -M^{-2}(1 + \nabla^2/M^2 + \ldots)\mathbb{1}$.

B. Pauli-Villars regularization

Feynman diagrams containing loops in general contain UV divergences which must be dealt with through the process of perturbative renormalization. For our purposes it is convenient to use Pauli-Villars (PV) renormalization [48]. In PV regularization we replace the original scalar Green's function $\Delta_\sigma(Z)$ with the regularized function

$$\Delta_\sigma^{\rm reg}(Z) := \Delta_\sigma(Z) + \sum_{i=1}^{[D/2]} C_i \Delta_{\rho_i}(Z). \tag{21}$$

Here $[\dots]$ denotes the integer part. This function is nothing more than the original Green's functions plus Green's functions of heavy particles with masses $M_i^2 = -\rho_i(\rho_i + 2\alpha)$. We take the masses M_i^2 to belong to the principal series so that $\Delta_\sigma^{\rm reg}(Z)$ will decay for large $|Z| > 1$ at the same rate as $\Delta_\sigma(Z)$. The coefficients C_i are bounded functions of the M_i^2 chosen to make $\Delta_\sigma^{\rm reg}(Z)$ finite at $Z = 1$; i.e., to cancel the UV-divergent terms in $\Delta_\sigma(Z)$ (including the logarithmic divergences that occur for even dimensions). For example, for $D = 2, 3$ the PV-regularized Green's function is

$$\Delta_\sigma^{\rm reg}(Z) = \Delta_\sigma(Z) - \Delta_\rho(Z), \quad \text{for } D = 2, 3 \tag{22}$$

while for $D = 4, 5$ it is

$$\Delta_\sigma^{\rm reg}(Z) := \Delta_\sigma(Z) + C_1 \Delta_{\rho_1}(Z) + C_2 \Delta_{\rho_2}(Z), \quad \text{for } D = 4, 5 \tag{23}$$

where the coefficients satisfy

$$C_1 + C_2 = -1, \quad C_1 M_1^2 + C_2 M_2^2 = -M^2. \tag{24}$$

One may write similar expressions for any dimension (see e.g. [48]) and, if desired, one may make further PV subtractions to ensure that $\Delta_\sigma^{\rm reg}(Z)$ is differentiable to any desired order at $Z = 1$. Such additional subtractions are useful in dealing with either field-renormalization counter-terms or derivatively coupled theories. Below, we assume for simplicity of notation that neither of these is present in our theory. However, the analysis is identical in the presence of derivative couplings so long as one assumes sufficient PV subtractions to have been made to render all diagrams finite at the desired order of perturbation theory[3]. In particular, detailed specification of these subtractions is not needed.

The cancellation of UV singularities has immediate implications for the Mellin-Barnes representation of the regulated propagators. Since the short-distance expansion is determined by the location of the right-poles, and since right poles with $\mathrm{Re}\nu < 0$ give terms divergent at $Z = 1$ (where the character of the divergence depends on the location of the pole), all such right-poles must cancel; i.e., the fundamental strip for the regularized propagators may be extended to $< \sigma, 0 >$ without picking up any explicit pole terms of the sort that appeared in (13). It follows that for any $\sigma < 0$ we may write the regularized Green's function as

$$\Delta_\sigma^{\rm reg}(Z) = \int_\nu \psi_\sigma^{\rm reg}(\nu) \Gamma(-\nu) \left(\frac{1-Z}{2}\right)^\nu \tag{25}$$

with

$$\psi_\sigma^{\rm reg}(\nu) := \psi_\sigma(\nu) + \sum_{i=1}^{[D/2]} C_i \psi_{\rho_i}(\nu). \tag{26}$$

The function $\psi_\sigma^{\rm reg}(\nu)$ is analytic on the interval $(\mathrm{Re}\,\sigma, \frac{1}{2})$ in odd dimensions and $(\mathrm{Re}\,\sigma, 1)$ in even dimensions. Using the results in appendix A one may readily show that the function $\psi_\sigma(\nu)$ – and therefore $\psi_\sigma^{\rm reg}(\nu)$ as well – has the asymptotic behavior

$$|\psi_\sigma(x+iy)| = e^{-3|y|/2} |y|^{-1+x} \left[1 + O\left(|y|^{-1}\right)\right] \quad \text{for } |y| \gg 1. \tag{27}$$

---

[3] For theories that are power-counting renormalizable, one may fix the set of PV subtractions independent of the order in perturbation theory. On the other hand, non-renormalizable theories should be treated as effective theories. In this case, there is no harm in taking the regularization scheme (i.e., the set of PV subtractions) to depend on the order in perturbation theory to which one works.

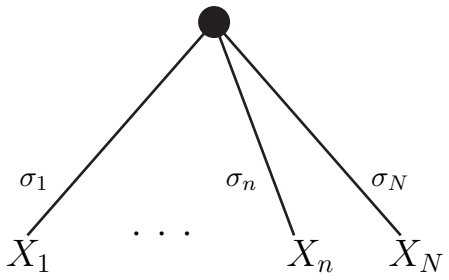

FIG. 3. The single-vertex tree Feynman diagram.

Furthermore, the integrand in (25) has only a simple pole at $\nu = 0$ which insures that there is no logarithmic UV divergence.

The PV-regularized Green's function $\Delta_\sigma^{\rm reg}(Z)$ is a bounded function of Z. Because the sphere is compact it follows that using the regularized Green's function to compute correlation functions yields regularized correlation functions that are bounded functions of the embedding distances. The UV divergences of the original perturbation series are recovered in the limit $M_i^2 \to +\infty$. We consider theories which can be renormalized by subtracting local counter-terms with coefficients depending on the regulator masses M_i. As remarked in footnote 2 above, one would expect this procedure to be equivalent (up to finite local counter-terms) to the renormalization prescription given in [35], and thus to define a fully covariant renormalized quantum field theory in the sense of [34] whenever the flat-space limit is power-counting renormalizable.

C. Single-vertex diagrams

In this section we compute the connected, single-vertex tree-level Feynman diagram that arises lowest order in perturbation theory; see Fig. 3. As stated in section III B, for simplicity of notation we assume below that there are derivative couplings. However, the analysis in the presence of derivative couplings is essentially identical.

We find it convenient to first use the PV-regulated Green's functions $\Delta_\sigma^{\rm reg}(Z)$ for our computation and then to take the limit where the regulators are removed. While such regularization is not in fact necessary for tree diagrams, it has the convenient property that it allows us to use the MB representation (25) which treats all masses uniformly. Our discussion below involves a set of fields with mass parameters σ_i. Note that each σ_i requires its own set of regulator masses M_{ij}, so removing the regulators is the limit $M_{ij} \to \infty$ (or $\rho_{ij} \to \infty$).

The diagram in Fig. 3 is given by the expression

$$\mathcal{V}_N(X_1, \ldots, X_n, X_N) = \int_Y \Delta_{\sigma_1}^{\rm reg}(X_1 \cdot Y) \cdots \Delta_{\sigma_n}^{\rm reg}(X_n \cdot Y) \Delta_{\sigma_N}^{\rm reg}(X_N \cdot Y). \tag{28}$$

Here Y is a unit vector and $\int_Y \ldots$ denotes an integral over S^D. To compute the right-hand side we first expand the Green's functions $\Delta_{\sigma_i}^{\rm reg}(X_i \cdot Y)$ according to (25):

$$\Delta_{\sigma_i}^{\rm reg}(X_i \cdot Y) = \int_{\nu_i} \psi_{\sigma_i}^{\rm reg}(\nu_i) \Gamma(-\nu_i) \left(\frac{1 - X_i \cdot Y}{2}\right)^{\nu_i}. \tag{29}$$

After inserting N copies of this into (28) the integral over Y becomes

$$\mathcal{M}_N := \int_Y \left(\frac{1 - X_1 \cdot Y}{2}\right)^{\nu_1} \cdots \left(\frac{1 - X_n \cdot Y}{2}\right)^{\nu_n} \left(\frac{1 - X_N \cdot Y}{2}\right)^{\nu_N}. \tag{30}$$

This master integral is performed in Appendix B; the result is

$$\mathcal{M}_N = \frac{(4\pi)^{\alpha+1/2}}{\Gamma\left[-\nu_1, \ldots, -\nu_n, -\nu_N, 1 + 2\alpha + \sum \nu_i\right]} \int_{(a)} \left\{ \left(\frac{1 - X_1 \cdot X_2}{2}\right)^{a_{12}} \cdots \left(\frac{1 - X_n \cdot X_N}{2}\right)^{a_{nN}} \right.$$
$$\left. \Gamma\left[-a_{12}, \ldots, -a_{nN}, A_1 - \nu_1, \ldots, A_N - \nu_N, \frac{1}{2} + \alpha + \sum \nu_i - \sum a_{ij}\right] \right\}. \tag{31}$$

Here $\int_{(a)} \dots$ denotes an integral over $N(N-1)/2$ integration variables a_{ij}. The a_{ij} are labelled according to the corresponding embedding distance $X_i \cdot X_j$. We use the shorthand $A_i = \sum_{j=1}^{N} a_{ij}$. The integration contours lie between their respective left and right poles. After performing the shift of variables $\nu_i \to \nu_i + A_i$ we obtain

$$\begin{aligned} &\langle \phi_{\sigma_1}(X_1) \cdots \phi_{\sigma_n}(X_n) \phi_{\sigma_N}(X_N) \rangle \\ &= \int_{(a)} \left\{ \left(\frac{1 - X_1 \cdot X_2}{2} \right)^{a_{12}} \cdots \left(\frac{1 - X_n \cdot X_N}{2} \right)^{a_{nN}} \Gamma\left[-a_{12}, \dots, -a_{nN} \right] V_N(a) \right\} \end{aligned} \tag{32}$$

with

$$\begin{aligned} V_N(a) = (4\pi)^{\alpha+1/2} \int_{[\nu]} \Bigg\{ &\Gamma\left[-\nu_1, \dots, -\nu_N \right] \psi^{\mathrm{reg}}_{\sigma_1}(A_1 + \nu_1) \cdots \psi^{\mathrm{reg}}_{\sigma_N}(A_N + \nu_N) \\ &\Gamma\left[\begin{array}{c} \frac{1}{2} + \alpha + \sum \nu_i + \sum a_{ij} \\ 1 + 2\alpha + \sum \nu_i + 2 \sum a_{ij} \end{array} \right] \Bigg\}. \end{aligned} \tag{33}$$

Our main task is to determine the fundamental strip of each a_{ij} variable. The Gamma functions in (32) restrict the fundamental strip of each a_{ij} variable to satisfy $\mathrm{Re}\, a_{ij} < 0$. To further determine the FS we must determine where the function $V_N(a)$ ceases to be analytic in the a_{ij}. When all a_{ij} satisfy $\mathrm{Re}\, a_{ij} \leq 0$ the function $V_N(a)$ imposes no further restriction on the right side of the fundamental strips. Because of the symmetry of the diagram we need only study one variable in detail, say a_{12}. As a function of a_{12} the function $V_N(a)$ has left poles at

$$a_{12} = \sigma_1 - A'_1 - n, \quad a_{12} = \sigma_2 - A'_2 - n, \quad a_{12} = -\frac{1}{2} - \alpha - \sum{}' a_{ij} - n. \tag{34}$$

In this expression $n \in \mathbb{N}_0$, $A'_1 = A_1 - a_{12}$, etc., and $\sum' a_{ij} = \sum a_{ij} - a_{12}$. We conclude that the FS of a_{12} is

$$a_{12} : < \max \left\{ \sigma_1 - A'_1, \sigma_2 - A'_2, -\frac{1}{2} - \alpha - \sum{}' a_{ij} \right\}, 0 > . \tag{35}$$

Analogous statements hold for the remaining a_{ij}. In (35) and below we take the operation max to select the greatest real part of any of its arguments. Note in particular that since the regulator masses M_{ij} lie in the principle series (so that Re $\rho_{ij} = -\alpha$ is fixed) the allowed strip (35) is independent of the values chosen for the regulator masses M_{ij}, though it does depend on the precise locations chosen for the other contours.

We can use our knowledge of the fundamental strips of the a_{ij} variables to bound the behavior of the diagram $\mathcal{V}_N$ at large embedding distances Z_{ij}. For example, consider the case $|Z_{12}| \gg 1$ and all other $Z_{ij} \neq 1$. We are free to arrange the a_{ij} integration contours such that all a_{ij} except a_{12} are fixed satisfying $\mathrm{Re}\, a_{ij} = -\epsilon$ where ϵ is an infinitesimal positive constant. In this configuration the FS of a_{12} becomes

$$a_{12} : < \max \left\{ \sigma_1, \sigma_2 \right\} + O(\epsilon), 0 > . \tag{36}$$

We can therefore move the a_{12} integration contour to $a_{12} = \max\{\sigma_1, \sigma_2\} + O(\epsilon)$. In this configuration it becomes clear that the diagram decays at least as fast as $|Z_{12}|^{\max\{\sigma_1,\sigma_2\}+O(\epsilon)}$. More generally we may say that when any embedding distance satisfies $|Z_{ij}| \gg 1$ the diagram decays at least as fast as $|Z_{ij}|^{\sigma_{\max}+O(\epsilon)}$ where $\sigma_{\max} = \max\{\sigma_1, \dots, \sigma_N\}$ and infinitesimal $\epsilon > 0$.

The diagram $\mathcal{V}_N$ provides the connected part of the PV-regulated N-point correlation function $\langle \phi_{\sigma_1}(X_1) \cdots \phi_{\sigma_n}(X_n) \phi_{\sigma_N}(X_N) \rangle$ to lowest order in perturbation theory. Our primary goal is to determine the behavior of such connected correlators when the operators are taken to large separations, so that several embedding distances Z_{ij} become large. From the discussion above it follows that the connected PV-regulated correlator decays at least as fast as $|Z|^{\sigma_{\max}+O(\epsilon)}$, where $|Z|$ is the largest embedding distance between operators. In practice the diagram may decay much more rapidly.

In order to show that the unregulated diagrams have the same IR behavior, we must take the limit $M_i^2 \to \infty$ where the regulator masses become large. The key step is to recall, as noted below (35), that the allowed locations of the a_{ij} contours are independent of the regulator masses M_{ij}. We may therefore investigate the large M_{ij} behavior by inserting the asymptotic expansion (17) for the $\psi_{\rho_{ij}}(A_i + \nu_i)$, associated with the propagators for the PV regulator masses, into (33) with the a_{12} contour fixed at any location allowed by (35) (and analogously for the other a_{ij}). To leading order, all dependence on the regulator masses is in factors of the form $(\rho_1)^{2\alpha-1+2A_1+2\nu_1}$. The particular power law depends on the location of the ν_i contours, and the most favorable behavior is obtained by taking the ν_i contours to be as far to the left as possible. With this in mind, taking into account certain relevant poles, it is straightforward to analyze the large M_{ij} behavior. The leading term is independent of M_{ij} and is obtained by simply replacing every

$\psi_\sigma^{\rm reg}$ with the unregulated ψ_σ; i.e., just by the unregulated expression. Sub-leading terms are suppressed by powers of M_{ij}^{-2} and can be neglected. Since the unregulated ψ_σ also satisfy (27) at large imaginary ν_i, the $\mathcal{O}(1)$ Mellin-Barnes integral can be analyzed in the usual way to find asymptotic behaviors at large $|Z_{ij}|$ dictated by the locations of the a_{ij} contours; i.e., by (35) and its analogues. Thus the large $|Z_{ij}|$ behavior of the $M_{ij} \to \infty$ limit satisfies the same bounds we derived at finite M_{ij}. In particular, the limiting diagram decays at least as fast as $|Z|^{\sigma_{\max}+O(\epsilon)}$, where $|Z|$ is the largest embedding distance between operators.

IV. GENERAL DIAGRAMS

In this section we analyze connected Feynman diagrams containing loops. We again use the PV-regulated propagators of section III B. For simplicity of notation we again assume that there are no derivative couplings or field-renormalization counter-terms. However, the analysis with derivative couplings or field-renormalization counter-terms is essentially identical so long as sufficient PV subtractions have been made as described in section III B.

At the technical level, the key step will be to show in section IV B that all diagrams have a Mellin-Barnes representation of the following form:

$$\begin{aligned}&\mathcal{V}_N(X_1,\dots,X_n,X_N)\\ &= \int_{(a)} \left\{ \left(\frac{1-X_1\cdot X_2}{2}\right)^{a_{12}} \cdots \left(\frac{1-X_n\cdot X_N}{2}\right)^{a_{nN}} \Gamma\left[-a_{12},\dots,-a_{nN}\right] V_N(a) \right\},\end{aligned} \tag{37}$$

where the function $V_N(a)$ satisfies the following requirements:

1. $V_N(a)$ is analytic when all a_{ij} are contained within the region given by the set of restrictions

$$\operatorname{Re} a_{ij} \in (\sigma_{\max} - \mathcal{P}_{ij}(a'), 0]. \tag{38}$$

   Here $\sigma_{\max}$ is the real part of the mass parameter of the lightest field participating in the diagram and $\mathcal{P}_{ij}(a')$ is a polynomial function of all the $\operatorname{Re} a_{kl}$ variables except $\operatorname{Re} a_{ij}$ (hence the prime) and has non-negative coefficients.

2. When the a_{ij} are contained in the region (38) the function $V_N(a)$ decays at large $|\operatorname{Im} a_{12}| \gg 1$ at least as rapidly as

$$|V_N(x+iy, a_{13},\dots,a_{nN})| \propto e^{-\pi|y|/2}|y|^{-1+x}, \quad \text{for } |y| \gg 1, \tag{39}$$

   and likewise for the other a_{ij}.

However, let us first discuss the implications of this form and show that it leads to exponentially decaying correlators as desired.

A. Implications of our Mellin-Barnes representation

To begin, note that the requirement (39) ensures that each integral in (37) converges so long as *no* embedding distance is equal to unity, i.e. when the diagram is evaluated away from coincident points. For any $a_{ij} = x + iy$ the integrand in (37) is comparable at large $|y| \gg 1$ to

$$e^{-\pi|y|+i\pi y}|y|^{3/2} \left|\frac{1-X_i\cdot X_j}{2}\right|^x, \tag{40}$$

and thus converges absolutely. To evaluate $\mathcal{V}(X_1,\dots,X_n,X_N)$ at coincident points we must move some of the contours into the right half-plane. For example, suppose we wish to evaluate $\mathcal{V}_N(X_1,\dots,X_n,X_N)$ at $X_1 = X_2$. To do so we first move the a_{12} contour into the right half-plane. In doing so pick up a residue from the pole at $a_{12} = 0$. From (38) it follows that $V_N(a_{12}=0,\dots)$ is regular and so this pole is a simple pole. Upon setting $X_1\cdot X_2 = 1$ the remaining

contour integral, with a_{12} (slightly) in the right half-plane vanishes, leaving just the residue:

$$\mathcal{V}_N(X_2, X_2, \ldots, X_n, X_N) = \int_{(a')} \Bigg\{ \left(\frac{1 - X_2 \cdot X_3}{2}\right)^{a_{13}+a_{23}} \cdots \left(\frac{1 - X_2 \cdot X_N}{2}\right)^{a_{1N}+a_{2N}} \left(\frac{1 - X_3 \cdot X_4}{2}\right)^{a_{34}} \cdots \left(\frac{1 - X_n \cdot X_N}{2}\right)^{a_{nN}} \Gamma\left[-a_{13}, \ldots, -a_{nN}\right] V_N(0, a_{13}, \ldots, a_{nN}) \Bigg\}. \tag{41}$$

Here $\int_{(a')} \ldots$ denotes that there is no a_{12} integral.

In fact, it turns out that the term on the right-hand side of (41) may be written in form (37), i.e. $\mathcal{V}_{N-1}(X_2, \ldots, X_N)$. Said differently, a function $\mathcal{V}_{N+K}(X_1, \ldots, X_N, X_{N+1}, \ldots, X_{N+K})$ when evaluated at $X_{N+1} = \cdots = X_{N+K} = Y$ is itself a function of the form $\mathcal{V}_{N+1}(X_1, \ldots, X_N, Y)$. For example, let us consider when $K = 2$. Following the procedure outlined above equation (41) we have

$$\mathcal{V}_{N+2}(X_1, \ldots, X_N, Y, Y) = \int_{(a')} \Bigg\{ \left(\frac{1 - X_1 \cdot X_2}{2}\right)^{a_{12}} \cdots \left(\frac{1 - X_n \cdot X_N}{2}\right)^{a_{nN}} \left(\frac{1 - X_1 \cdot Y}{2}\right)^{a_{1,N+1}+a_{1,N+2}} \cdots \left(\frac{1 - X_N \cdot Y}{2}\right)^{a_{N,N+1}+a_{N,N+2}} \Gamma\left[-a_{12}, \ldots, -a_{N,N+2}\right] V_{N+2}(a_{12}, \ldots, a_{N,N+2}, 0) \Bigg\}. \tag{42}$$

In this expression the prime in the (a') below the integral means that there is no $a_{N+1,N+2}$ integration. The integrand in (42) is still analytic with respect to the remaining a_{ij} in the region given by (38). It follows that after a few cosmetic changes we may write (42) in the form of (37). Let us re-label the variables $a_{i,N+2} \to c_i$ (here $i = 1, \ldots, N$), then shift variables $a_{i,N+1} \to a_{i,N+1} - c_i$; (42) becomes

$$\begin{aligned} &\mathcal{V}_{N+2}(X_1, \ldots, X_N, Y, Y) \\ &= \int_{(a)} \Bigg\{ \left(\frac{1 - X_1 \cdot X_2}{2}\right)^{a_{12}} \cdots \left(\frac{1 - X_n \cdot X_N}{2}\right)^{a_{nN}} \left(\frac{1 - X_1 \cdot Y}{2}\right)^{a_{1,N+1}} \left(\frac{1 - X_N \cdot Y}{2}\right)^{a_{N,N+1}} \\ &\qquad \Gamma\left[-a_{12}, \ldots, -a_{N,N+1}\right] V^{\text{new}}_{N+1}(a) \Bigg\}. \end{aligned} \tag{43}$$

In this expression the integral is over the variables $a_{12}, \ldots, a_{N,N+1}$ and $V^{\text{new}}_{N+1}(a)$ is given by

$$V^{\text{new}}_{N+1}(a) := \frac{1}{\Gamma\left[-a_{1,N+1}, \ldots, -a_{N,N+1}\right]} \int_{[c]} \Bigg\{ \Gamma\left[c_1 - a_{1,N+1}, \ldots, c_N - a_{N,N+1}, -c_1, \ldots, -c_N\right] V_{N+2}(a_{12}, \ldots, a_{nN}, c_1 - a_{1,N+1}, \ldots, c_N - a_{N,N+1}, c_1, \ldots, c_N, 0) \Bigg\}. \tag{44}$$

In this expression $\int_{[c]} \ldots$ denotes contour integration over $c_1, \ldots, c_N$. These integrals are guaranteed to converge so long as the a_{ij} are within the region for which the integrand of (42) is analytic. Although this expression is rather complicated, it is easy to verify that this function satisfies requirements (1) and (2) using the asymptotics described in appendix A. The same analysis may be performed for any $K > 1$ with the same conclusion: the function $\mathcal{V}_{N+K}(X_1, \ldots, X_N, Y, \ldots, Y)$ is of the form of a function $\mathcal{V}_{N+1}(X_1, \ldots, X_N, Y)$ given by (37).

The last and most important consequence of the form (37) is that the function $\mathcal{V}_N(X_1, \ldots, X_n, X_N)$ decays exponentially when evaluated at large embedding distances. For example, suppose $|X_1 \cdot X_2| \gg 1$. A bound on the decay of $\mathcal{V}_N(X_1, \ldots, X_n, X_N)$ can be found in the same manner as in the previous section. Let all integration contours except that of a_{12} be located at $\operatorname{Re} a_{ij} = -\epsilon$. From (38) it follows that in this configuration a_{12} has a fundamental strip at least as large as

$$a_{12} : < \sigma_{\max} + O(\epsilon), 0 >, \tag{45}$$

so $\mathcal{V}_N(X_1, \ldots, X_n, X_N)$ decays at least as fast as $(X_1 \cdot X_2)^{\sigma_{\max}+\epsilon}$ for any $\epsilon > 0$.

Furthermore, suppose that removing some vertex results in a disconnected diagram, and suppose also that one of the resulting connected components contains none of the original external legs. Then this piece contributes only an

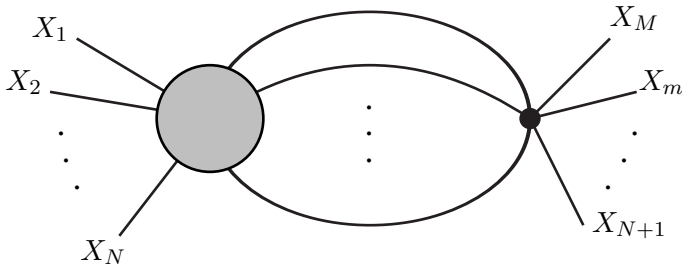

FIG. 4. The process of adding a new vertex to an existing diagram.

overall multiplicative constant (which is finite at finite regulators masses M_{ij}) to the diagram and does not affect the large Z behavior. One may therefore remove such pieces from the diagram when computing $\sigma_{\max}$ above. We refer to this process as "trimming," so that the trimmed version of a given diagram has all such pieces removed.

Obviously, the same result also holds for the other embedding distances. From this result it follows that the connected part of a PV-regulated N-point function – which may be described to any order in perturbation theory by diagrams of the form $\mathcal{V}_N$ – decays when any two operators are taken to be separated by a large distance Z at least as fast as $|Z|^{\sigma_{\max}+O(\epsilon)}$, where $\sigma_{\max}$ is the (real part of the) largest σ that appears in any trimmed diagram that contributes to the correlator.

B. Proof of the desired Mellin-Barnes representation

The proof that all diagrams can be written in the form (37) is through induction. One constructs a diagram vertex by vertex, beginning with a single-vertex tree diagram. We have already seen that single-vertex diagrams have MB integral representations of the required form. Thus one simply needs to show that, upon adding a vertex to an existing diagram with the form (37), the new diagram is again of the form (37). We show this below.

The process of adding a new vertex to an existing diagram is shown schematically in Fig 4.Starting with an $(N+K)$-legged diagram $\mathcal{V}_{N+K}(X_1,\ldots,X_N,X_{N+1},\ldots,X_{N+K})$, one attaches a new vertex to the $K\geq 1$ external legs $X_{N+1},\ldots,X_{N+K}$. One then attaches to the new vertex $(M-N)$ new external legs so that the new diagram is an M-legged diagram:

$$\mathcal{V}_M(X_1,\ldots,X_M)=\int_Y \mathcal{V}_{N+K}(X_1,\ldots,X_N,Y,\ldots,Y)\Delta^{\rm reg}_{\sigma_{N+1}}(X_{N+1}\cdot Y)\cdots\Delta^{\rm reg}_{\sigma_M}(X_M\cdot Y). \tag{46}$$

This procedure generates all diagrams in which no propagator has both of its ends on the same vertex. But adding such one-link loops simply multiplies any diagram by factors of $\Delta^{\rm reg}_\sigma(Y\cdot Y)$, which are just finite constants due to our PV regularization, and which are readily absorbed into the definition of $\mathcal{V}_M$. It thus remains only to show that the diagrams generated by the above process satisfy requirements (1) and (2) associated with (37).

Note that $K\geq 1$ in order for the diagram to be connected. Following the discussion in section IV A, since $K\geq 1$ we know that $\mathcal{V}_{N+K}(X_1,\ldots,X_N,Y,\ldots,Y)$ can be written in the form of some $\mathcal{V}_{N+1}(X_1,\ldots,X_N,Y)$. Inserting this (46) becomes

$$\mathcal{V}_M(X_1,\ldots,X_M)=\int_Y \mathcal{V}_{N+1}(X_1,\ldots,X_N,Y)\Delta^{\rm reg}_{\sigma_{N+1}}(X_{N+1}\cdot Y)\cdots\Delta^{\rm reg}_{\sigma_M}(X_M\cdot Y). \tag{47}$$

It is convenient to define $n=N-1$ and $m=M-1$. The integral (46) can be computed in essentially the same manner as the single-vertex diagram section III. We begin by expressing both $\mathcal{V}_{N+1}(X_1,\ldots,X_N,Y)$ and the regulated Green's functions in terms of their MB integral representations:

$$\begin{aligned}&\mathcal{V}_{N+1}(X_1,\ldots,X_N,Y)\\ &=\int_{(a)}\int_{\nu_1}\cdots\int_{\nu_N}\left\{\left(\frac{1-X_1\cdot X_2}{2}\right)^{a_{12}}\cdots\left(\frac{1-X_n\cdot X_N}{2}\right)^{a_{nN}}\left(\frac{1-X_1\cdot Y}{2}\right)^{\nu_1}\cdots\left(\frac{1-X_N\cdot Y}{2}\right)^{\nu_N}\right.\\ &\left.\Gamma\left[-a_{12},\ldots,-a_{nN},-\nu_1,\ldots,-\nu_N\right]V_{N+1}(a_{12},\ldots,a_{nN},\nu_1,\ldots,\nu_N)\right\},\end{aligned} \tag{48}$$

$$\Delta^{\rm reg}_{\sigma_i}(X_i\cdot Y)=\int_{\nu_i}\psi^{\rm reg}_{\sigma_i}(\nu_i)\Gamma\left(-\nu_i\right)\left(\frac{1-X_i\cdot Y}{2}\right)^{\nu_i}. \tag{49}$$

Here it is important to keep track of notation. In the first equation we have relabelled $a_{i,N+1}\to\nu_i$, $i=1,\ldots,N$, so that the remaining $N(N-1)/2$ a_{ij} variables run $a_{12},\ldots,a_{nN}$. In the second expression i runs $i=N+1,\ldots,M$. Inserting these into (47) we then integrate over Y using the master integral $\mathcal{M}_M$ (see (31)). After performing a shift of integration variables $\nu_i\to\nu_i+B_i$ (where $B_i=\sum_{j=1}^N b_{ij}$) we arrive at

$$\begin{aligned}\mathcal{V}_M(X_1,\ldots,X_M)=&\int_{(a)}\int_{(b)}\left\{\left(\frac{1-X_1\cdot X_2}{2}\right)^{a_{12}+b_{12}}\cdots\left(\frac{1-X_n\cdot X_N}{2}\right)^{a_{nN}+b_{nN}}\right.\\&\left.\left(\frac{1-X_1\cdot X_{N+1}}{2}\right)^{b_{1,N+1}}\cdots\left(\frac{1-X_m\cdot X_M}{2}\right)^{b_{mM}}\Gamma\left[-a_{12},\ldots,-a_{nN},-b_{12},\ldots,-b_{mM}\right]V_M(a,b)\right\}.\end{aligned} \tag{50}$$

In this expression the b_{ij} run over all distinct pairs ij (i.e., $b_{12},\ldots,b_{mM}$) and

$$\begin{aligned}V_M(a,b)=\int_{[\nu]}\left\{\Gamma\left[\begin{array}{c}-\nu_1,\ldots,-\nu_M,\frac{1}{2}+\alpha+\sum\nu_i+\sum b_{ij}\\1+2\alpha+\sum\nu_i+2\sum b_{ij}\end{array}\right]\right.\\\left.V_{N+1}(a_{12},\ldots,a_{nN},B_1+\nu_1,\ldots,B_N+\nu_N)\psi^{\rm reg}_{\sigma_{N+1}}(B_{N+1}+\nu_{N+1})\cdots\psi^{\rm reg}_{\sigma_M}(B_M+\nu_M)\right\}.\end{aligned} \tag{51}$$

It is now straightforward to determine the region for which the integrand in (50) is analytic in the integration variables. The simplest variables to analyse are the b_{ij} variables with $N<i,j\leq M$. For these variables the analysis is identical to that performed for the single-vertex graph; the result is that the integrand is analytic in the region

$$\text{Re }b_{mM}\in\left(\max\left\{\sigma_m-B'_m,\sigma_M-B'_M,-\frac{1}{2}-\alpha-\sum{}'b_{ij}\right\},0\right]. \tag{52}$$

As usual here the prime denotes that b_{mM} is omitted from the sums. For variables b_{ij} with $1\geq i\leq N$ and $N<j\leq M$ one finds

$$\text{Re }b_{1M}\in\left(\max\left\{\sigma_{\max}-\mathcal{P}_{1,N+1}(a,b),\sigma_M-B'_M,-\frac{1}{2}-\alpha-\sum{}'b_{ij}\right\},0\right]. \tag{53}$$

Finally, let us determine the region for which the integrand is analytic with respect to a_{ij} while holding the b_{ij} contours with $1\leq i,j\leq N$ fixed to satisfy $\text{Re}\,b_{ij}=-\epsilon$. In this configuration it is easy to determine that the integrand is analytic when

$$\text{Re }a_{12}\in\left(\sigma_{\max}-\mathcal{P}_{12}(a,b)+O(\epsilon),0\right]. \tag{54}$$

Therefore, we can perform the shift of variables $a_{ij}\to a_{ij}-b_{ij}$ in order to get (50) in the form (37). We know that the b_{ij} integrals with $1\leq i,j\leq N$ will converge in the region given by (52)-(54). We see that (52)-(54) satisfy (38), and that all integrals converge sufficiently rapidly to satisfy (39). Thus we have shown that $\mathcal{V}_M(X_1,\ldots,X_M)$ is of the form 37.

C. Removing the regulator: the limit $M_{ij}^2\to\infty$

Our analysis above is complete at the level of effective theories. In that context, one keeps the regulators masses M_{ij} finite and is careful to ask questions only about physics at energy scales much less than M_{ij}. But for renormalizable theories one would like to do more and to remove the regulators by sending $M_{ij}\to\infty$ before taking the limit of large $|Z_{ij}|$.

Such questions are straightforward to address using our Mellin-Barnes representations. Note that, as with the tree diagrams discussed in section III C, we may study the large M_{ij} limit holding fixed the locations of all contours, subject only to the conditions (38) found above. Suppose for the moment that we choose the couplings to be independent of the regulators masses M_{ij}. Then all of the regulator-dependence lies in the functions $\psi_\rho(\nu)$ associated with the

regulator Green's functions and the coefficients C_i. Note that each term in the asymptotic expansion (17) of such functions at large M_{ij} again decays exponentially away from the real axis (now roughly as $e^{-\pi|y|}$) fast enough for the arguments of sections IV A,IV B to hold[4]. As a result, inserting the expansion (17) into one of our Mellin-Barnes integrals (and also expanding the C_i) produces an asymptotic series in the masses M_{ij}, each of whose coefficients is again a Mellin-Barnes integral with the same contours and convergence properties as the original expression.

Of course, the above expansion will in general include positive powers of M_{ij} as well as negative powers; these are just the expected ultra-violet divergences of the theory. But let us suppose that by taking the coupling constants to depend on M_{ij} in an appropriate way the $M_{ij} \to \infty$ limits of correlators become well-defined and finite, at least to some fixed order in perturbation theory. This is precisely the assumption that the divergences can be cancelled by some set of M_{ij}-dependent counter-terms. Since coupling constants are just overall multiplicative factors in each diagram, it is straightforward to take this extra dependence on the M_{ij} into account. Expanding each coupling in an asymptotic series generates a new series, where each term is again a Mellin-Barnes integral of our standard form (and with the same placement of the contours). This is true in particular of the term that is independent of the M_{ij}. But this term gives the full $M_{ij} \to \infty$ limit, since all terms involving positive powers of M_{ij} must have cancelled in order to obtain a finite result. The usual argument then implies that this term decays as $|Z|^{\sigma_{\max}+\mathcal{O}(\epsilon)}$ at large $|Z|$, where $\sigma_{\max}$ is the (real part of the) largest σ that appears in any trimmed diagram that contributes to the correlator at this order. We will provide an explicit example of this renormalization procedure in a future publication [49].

V. DISCUSSION

In the above work, we used Mellin-Barnes techniques to determine the asymptotics of Pauli-Villars regulated diagrams for massive scalar quantum field theories in de Sitter space. We found that connected correlators fall off at large $|Z|$ at least as fast as does the Green's function for the lightest field in the (trimmed) diagram (up to corrections that grow less strongly than powers laws; e.g., factors of $\log|Z|$). Due to the simple way in which changing the PV regulator masses interacted with the Mellin-Barnes expressions, it was straightforward to show that the same results hold in the $M_{ij} \to \infty$ limit in which the regulators are removed, independent of the details of any counter-terms required. An explicit example of this renormalization procedure will appear in [49]. A similar analysis using Mellin-Barnes techniques should also be possible in the context of dimensional regularization.

As described in the introduction, for the (massive scalar) QFTs considered it follows that, for any state obtained by acting with appropriate smeared field operators on the Hartle-Hawking vacuum, any correlation function will approach that of the Hartle-Hawking vacuum at large times; i.e., that the interacting Hartle-Hawking vacuum is an attractor state in the sense of [27] for local correlators at any order of perturbation theory. Since the above class of states includes any perturbation of the Hartle-Hawking vacuum created by a source of compact support, this provides a sense in which this vacuum is stable despite the possible concerns raised in e.g. [30, 31, 33].

Our results hold for all masses $M^2 > 0$ for which a free Euclidean vacuum exists and for arbitrary interactions, with non-renormalizable theories being treated as effective theories. While for simplicity of notation the calculations were presented only for non-derivative couplings, no significant changes are required to analyze derivatively-coupled theories and (as usual) derivatives can only strengthen the fall-off at large Z. It would be very interesting if our results could be extended to the massless case $M^2 = 0$ following e.g. the approach of [50], which introduced a new form of perturbation theory on S^D.

Some readers may be concerned by our use of Euclidean techniques. But on general grounds the Hartle-Hawking state should be a valid quantum state. In particular, the analytically continued correlators satisfy the Lorentz-signature Schwinger-Dyson equations. Furthermore, the de Sitter analogue [51] of the Osterwalder-Schräder construction implies that the Hartle-Hawking state lives in a positive-definite Hilbert space whenever the Euclidean correlators satisfy reflection-positivity. This in turns holds at least formally whenever the Euclidean action is bounded below, and has been rigorously shown in $D = 2$ dimensions for standard kinetic terms and polynomial potentials; see e.g. [52]. In such cases, it remains only to ask how the Hartle-Hawking state relates to other states of interest; e.g, perhaps the state defined by the standard in-in perturbation theory in the expanding cosmological patch of dS_D. This question will be investigated in detail in [53], where it will be shown that these two states agree for massive scalar fields.

It would be interesting to apply some version of these tools to massless scalar fields, perhaps using the perturbation scheme described in [50]. Although the natural propagator of this scheme grows logarithmically at large Z due to a double pole at the origin, it is possible that this behavior will softened by higher order corrections. Finally, we emphasize that we consider field theories on a fixed spacetime background in which the metric is non-dynamical. As

[4] In fact, such arguments require decay only as $e^{-\pi|y|/2}$ times an appropriate power law or faster.

the known propagators for gravitons do not fall off at large separations, the situation for dynamical gravity may be quite different.

ACKNOWLEDGMENTS

The authors thank David Berenstein, Cliff Burgess, Steven B. Giddings, Atsushi Higuchi, Stefan Hollands, Alexander Polyakov, Mark Srednicki, and Richard Woodard for enlightening discussions. This work was supported in part by the US National Science Foundation under grants PHY05-55669 and PHY08-55415 and by funds from the University of California.

Appendix A: Mellin-Barnes integrals

We write a generic Mellin-Barnes integral as [5]

$$f(Z) = \int_\nu \Gamma \left[\begin{array}{c} a_1 + A_1\nu, \ldots, a_m + A_m\nu, b_1 - B_1, \ldots, b_n - B_n\nu \\ c_1 + C_1\nu, \ldots c_p + C_p\nu, d_1 - D_1\nu, \ldots, d_q - D_q\nu \end{array} \right] (Z)^\nu, \tag{A1}$$

where the measure $d\nu/2\pi i$ is implicit and the contour is a straight line parallel to the imaginary axis, traversed from $-i\infty$ to $+i\infty$, lying between the left and right poles. The convergence of the integral (A1) is governed by the behavior of the integrand at large $|\mathrm{Im}\ \nu|$. This behavior can be determined from the well-known asymptotic behavior of the Gamma function:

$$\lim_{|y|\to\infty} \Gamma(x+iy) = (2\pi)^{1/2} e^{-\frac{\pi}{2}|y|} |y|^{x-1/2} \left[1 + O(y^{-1})\right]. \tag{A2}$$

Let us assume that the all A_i, B_i, C_i, D_i are positive and define

$$E = \sum_{i=1}^m A_i + \sum_{i=1}^n B_i - \sum_{i=1}^p C_i - \sum_{i=1}^q D_i, \tag{A3}$$

$$F = \sum_{i=1}^m A_i - \sum_{i=1}^n B_i - \sum_{i=1}^p C_i + \sum_{i=1}^q D_i, \tag{A4}$$

$$G = \mathrm{Re}\left[\sum_{i=1}^m a_i + \sum_{i=1}^n b_i - \sum_{i=1}^p c_i - \sum_{i=1}^q d_i\right] + \frac{1}{2}(-m-n+p+q), \tag{A5}$$

$$H = \prod_{i=1}^m (A_i)^{A_i} \prod_{i=1}^n (B_i)^{-B_i} \prod_{i=1}^p (C_i)^{-C_i} \prod_{i=1}^q (D_i)^{D_i}, \tag{A6}$$

and furthermore let $Z = Re^{i\Phi}$ and $\nu = x + iy$. With this notation the absolute value of the integrand behaves like

$$\exp\left[-\Phi y - \frac{E\pi}{2}|y|\right] |y|^{Fx+G} (RH)^x \tag{A7}$$

as $|y| \to \infty$. From this we conclude that the integral (A1) is absolutely convergent when

1. $|\Phi| < E\pi/2$. The integral A1 defines an analytic function of Z for $|\arg Z| < \min\left(\pi, \frac{E\pi}{2}\right)$.

2. $|\Phi| = E\pi/2$ and $Fx + G < -1$. The integral defines an analytic function for all Z.

See [54] for further details.

---

[5] This discussion follows closely the discussion in [54].

Appendix B: Calculation of $\mathcal{M}_N$

In this appendix we compute the integral

$$\mathcal{M}_N := \mathcal{M}(\nu_1, \ldots, \nu_N) = \int_Y \left(\frac{1 - X_1 \cdot Y}{2}\right)^{\nu_1} \cdots \left(\frac{1 - X_n \cdot Y}{2}\right)^{\nu_n} \left(\frac{1 - X_N \cdot Y}{2}\right)^{\nu_N} \tag{B1}$$

with $n = N - 1$. Rather than directly evaluating (B1) we instead consider the integral

$$\mathcal{A}(\alpha_1, \ldots, \alpha_n) := \int_Y \left[\alpha_1 \left(\frac{1 - X_1 \cdot Y}{2}\right) + \cdots + \alpha_n \left(\frac{1 - X_n \cdot Y}{2}\right) + \left(\frac{1 - X_N \cdot Y}{2}\right)\right]^{\lambda}, \tag{B2}$$

where α_i are arbitrary real parameters and λ is a complex number with $\operatorname{Re}\lambda < 0$. The quantities $\mathcal{A}$ and $\mathcal{M}$ may be related in a simple way. To do so we use a standard Mellin-Barnes formula:

$$\begin{aligned}&(A_1 + \cdots + A_n + A_N)^{\lambda} \\ &= \frac{1}{\Gamma(-\lambda)} \int_{u_1} \cdots \int_{u_n} \Gamma\left[-\lambda + \sum_{i=1}^{n} u_n,\, -u_1, \ldots,\, -u_n\right] (A_1)^{u_1} \cdots (A_n)^{u_n} (A_N)^{\lambda - \sum u_i}.\end{aligned} \tag{B3}$$

Inserting (B3) in (B2) yields

$$\begin{aligned}\mathcal{A}(\alpha_1, \ldots, \alpha_n) = \frac{1}{\Gamma(-\lambda)} \int_{u_1} (\alpha_1)^{u_1} \cdots \int_{u_n} (\alpha_n)^{u_n} \Bigg\{ &\Gamma\left[-\lambda + \sum_{i=1}^{n} u_i,\, -u_1,\, \ldots,\, -u_n\right] \\ &\mathcal{M}\left(u_1, \ldots, u_n, \lambda - \sum_{i=1}^{n} u_i\right)\Bigg\}.\end{aligned} \tag{B4}$$

Written this way $\mathcal{M}$ is one factor of the Mellin transform of $\mathcal{A}$.

Let us now return to (B2) and integrate over Y. We use the formula

$$\eta^{\lambda} = \frac{i^{-\lambda}}{\Gamma(-\lambda)} \int_0^{\infty} d\beta\, \beta^{-1-\lambda} e^{-i\beta\eta} \tag{B5}$$

to write $\mathcal{A}$ as

$$\mathcal{A}(\alpha_1, \ldots, \alpha_n) = \frac{(2i)^{-\lambda}}{\Gamma(-\lambda)} \int_0^{\infty} d\beta\, \beta^{-1-\lambda} \exp\left[-i\beta\left(1 + \sum_{i=1}^{n} \alpha_i\right)\right] \int_Y e^{+i\beta V Y} \tag{B6}$$

where $V = \alpha_1 X_1 + \cdots + a_n X_n + X_N$. The integral over Y can be written in terms of the Bessel function:

$$\int_Y e^{-i\beta V Y} = (2\pi)^{\alpha+1} \frac{J_{\alpha}(\beta|V|)}{(\beta|V|)^{\alpha}}. \tag{B7}$$

The Bessel function may be written as a Mellin-Barnes integral

$$J_{\nu}(z) = \int_{\mu} \Gamma\left[\begin{array}{c} -\mu \\ 1 + \nu + \mu \end{array}\right] \left(\frac{z}{2}\right)^{\nu + 2\mu}; \tag{B8}$$

inserting (B8) into (B7) yields

$$\int_Y e^{-i\beta V Y} = 2\pi^{\alpha+1} \int_{\mu} \Gamma\left[\begin{array}{c} -\mu \\ 1 + \alpha + \mu \end{array}\right] \left(\frac{\beta^2 V^2}{4}\right)^{\mu}. \tag{B9}$$

After inserting (B9) into (B6) we may integrate over β using the inverse of (B5)

$$\int_0^{\infty} d\beta\, \beta^{-1-\lambda} e^{-i\beta\eta} = \frac{\Gamma(-\lambda)}{i^{-\lambda}} (\eta - i0)^{\lambda}. \tag{B10}$$

Convergence of the integral over β requires $\mathrm{Re}\,(\lambda-2\mu)<0$. The result is

$$\mathcal{A}(\alpha_1,\ldots,\alpha_n)=\frac{2^{1-\lambda}\pi^{\alpha+1}}{\Gamma\,(-\lambda)}\int_\mu \Gamma\left[\begin{array}{c}-\mu,\,2\mu-\lambda\\1+\alpha+\mu\end{array}\right](2i)^{-2\mu}(V^2)^\mu\left(1+\sum_{i=1}^n\alpha_i\right)^{\lambda-2\mu}. \tag{B11}$$

Next we perform a number of manipulations in order to tidy up (B11). First note that

$$\begin{aligned}V^2&=\alpha_1^2+\cdots+\alpha_n^2+1+\alpha_1\alpha_2X_1X_2+\cdots+\alpha_nX_nX_N\\&=\left(1+\sum_{i=1}^n\alpha_i\right)^2+2\alpha_1\alpha_2(X_1X_2-1)+\cdots+2\alpha_n(X_nX_N-1).\end{aligned} \tag{B12}$$

It is convenient to use B3 to write

$$\begin{aligned}(V^2)^\mu=\frac{1}{\Gamma\,(-\mu)}\int_w\Bigg\{&\Gamma\,[-\mu+w,\,-w]\left(1+\sum_{i=1}^n\alpha_i\right)^{2(\mu-w)}\\&[2\alpha_1\alpha_2(X_1\cdot X_2-1)+\cdots+2\alpha_n(X_nX_N-1)]^w\Bigg\}.\end{aligned} \tag{B13}$$

Inserting this into (B11) yields

$$\begin{aligned}\mathcal{A}(\alpha_1,\ldots,\alpha_n)=\frac{2^{1-\lambda}\pi^{\alpha+1}}{\Gamma\,(-\lambda)}\int_\mu\int_w\Bigg\{&\Gamma\left[\begin{array}{c}2\mu-\lambda,\,-\mu+w,\,-w\\1+\alpha+\mu\end{array}\right](2i)^{-2\mu}\left(1+\sum_{i=1}^n\alpha_i\right)^{\lambda-2w}\\&[2\alpha_1\alpha_2(X_1X_2-1)+\cdots+2\alpha_n(X_nX_N-1)]^w\Bigg\}\end{aligned} \tag{B14}$$

We can now integrate over μ. First we use the Gamma function duplication formula

$$\Gamma\left[x,\,x+\frac{1}{2}\right]=2^{1-2x}\sqrt{\pi}\Gamma\,(2x) \tag{B15}$$

on the Gamma function $\Gamma\,(2\mu-\lambda)$; second we use the Gauss summation formula [54] written here as a Mellin-Barnes integral:

$$\int_\mu\Gamma\left[\begin{array}{c}a+\mu,\,b+\mu,\,d-\mu\\c+\mu\end{array}\right]e^{\pm i\pi\mu}=e^{\pm i\pi d}\,\Gamma\left[\begin{array}{c}a+d,\,b+d,\,c-a-b-d\\c-a,\,c-b\end{array}\right], \tag{B16}$$

valid for $\mathrm{Re}\,(c-a-b-d)>0$. Cleaning up we have

$$\begin{aligned}\mathcal{A}(\alpha_1,\ldots,\alpha_n)=\frac{2^{1+2\alpha}\pi^{\alpha+1/2}}{\Gamma\,[-\lambda,\,1+2\alpha+\lambda]}\int_w\Bigg\{&\Gamma\left[2w-\lambda,\,\frac{1}{2}+\alpha+\lambda-w,\,-w\right]\\&\left(1+\sum_{i=1}^n\alpha_i\right)^{\lambda-2w}\left[\alpha_1\alpha_2\left(\frac{1-X_1\cdot X_2}{2}\right)+\cdots+\alpha_n\left(\frac{1-X_nX_N}{2}\right)\right]^w\Bigg\}.\end{aligned} \tag{B17}$$

The next series of steps is simple but rather cumbersome to transcribe. We expand both the term in parentheses and the term in square brackets in (B17) using the Mellin-Barnes expansion (B3). Within the parentheses there are $n+1$ terms, so the Mellin-Barnes expansion of this quantity has n integrations. Likewise, the term in square brackets has $N(N-1)/2$ terms so the Mellin-Barnes expansion of this quantity has $N(N-3)/2$ integrations. After performing some shifts in the integration variables (taking care not to shift a contour through a pole) and relabelling we obtain

the following expression:

$$\begin{aligned}
&\mathcal{A}(\alpha_1,\ldots,\alpha_n) = \\
&= \frac{2^{1+2\alpha}\pi^{\alpha+1/2}}{\Gamma\left[-\lambda,\, 1+2\alpha+\lambda\right]} \int_{\mu_1} (\alpha_1)^{\mu_1} \cdots \int_{\mu_n} (\alpha_n)^{\mu_n} \Bigg\{ \\
&\int_{h_{12}} \cdots \int_{h_{nN}} \left\{ \left(\frac{1-X_1\cdot X_2}{2}\right)^{h_{12}} \cdots \left(\frac{1-X_n\cdot X_N}{2}\right)^{h_{nN}} \Gamma\left[-h_{12},\ldots,-h_{nN}\right] \right. \\
&\left. \Gamma\left[\sum h_{1i}-\mu_1,\, \ldots,\, \sum h_{ni}-\mu_n,\, \sum h_{Ni}-\lambda+\sum_{i=1}^{n}\mu_i,\, \frac{1}{2}+\alpha+\lambda-\sum h_{ij}\right] \right\} \Bigg\}.
\end{aligned} \tag{B18}$$

In this expression there is a total of n integration variables $\mu_1,\ldots,\mu_n$ and $N(N-1)/2$ variables h_{ij}. The latter are labelled such that each factor of $(1-X_i\cdot X_j)/2$ is raised to the power h_{ij}.

The convergence of each Mellin-Barnes integral may be evaluated using the technique described in Appendix A. Each integral converges absolutely for all $(1-X_i\cdot X_j)/2 \neq 1$. The expression (B18) defines a single-valued function of the inner products $X_i\cdot X_j$ for all complex values of $X_i\cdot X_j$ away from the cuts $X_i\cdot X_j \in [1,\infty)$.

Both (B4) and (B18) equate $\mathcal{A}$ with an n-fold Mellin transform with parameters α_i. It is easy to see that the integration contours of the two expressions – those of the u_i in the former expression and μ_i in the latter expression – may be taken to be traversed in the same places in their respective complex planes. Now recall that the Mellin inversion theorem states that for a given choice of integration contour the Mellin transform of a function is unique [54]. It follows that we may identify the integrands and equate $u_1=\mu_1,\ \ldots,\ u_n=\mu_n$. The final step is to relabel

$$\mu_i = u_i \to \nu_i, \quad \text{for } i=1,\ldots,n, \quad \lambda \to \nu_N + \sum_{i=1}^{n}\nu_i, \quad h_{ij}\to a_{ij}, \tag{B19}$$

which yields

$$\begin{aligned}
&\mathcal{M}(\nu_1,\ldots,\nu_N) \\
&= \frac{(4\pi)^{\alpha+1/2}}{\Gamma\left[-\nu_1,\ldots,-\nu_N,1+2\alpha+\sum\nu_i\right]} \int_{(a)} \left\{ \left(\frac{1-X_1\cdot X_2}{2}\right)^{a_{12}} \cdots \left(\frac{1-X_n\cdot X_N}{2}\right)^{a_{nN}} \right. \\
&\left. \Gamma\left[-a_{12},\ldots,-a_{nN},A_1-\nu_1,\ldots,A_N-\nu_N,\frac{1}{2}+\alpha+\sum\nu_i-\sum a_{ij}\right] \right\}.
\end{aligned} \tag{B20}$$

In this expression $A_i := \sum_{j=1}^{N} a_{ij}$.

---

[1] B. Allen, Phys. Rev., **D32**, 3136 (1985).
[2] A. A. Starobinsky, JETP Lett., **30**, 682 (1979).
[3] E. Mottola, Phys. Rev., **D31**, 754 (1985).
[4] E. Mottola, in *Physical Origins of Time Asymmetry*, edited by J. J. Halliwel, J. Pérez-Mercader, and W. H. Zurek (1994) pp. 504–515.
[5] I. Antoniadis, P. O. Mazur, and E. Mottola, New J. Phys., **9**, 11 (2007), arXiv:gr-qc/0612068.
[6] E. Mottola, Submitted to Acta Physica Polonica (2010), arXiv:1008.5006 [gr-qc].
[7] B. L. Hu and D. J. O'Connor, Phys. Rev. Lett., **56**, 1613 (1986).
[8] B. L. Hu and D. J. O'Connor, Phys. Rev., **D36**, 1701 (1987).
[9] N. C. Tsamis and R. P. Woodard, Phys. Lett., **B301**, 351 (1993).
[10] N. C. Tsamis and R. P. Woodard, Ann. Phys., **238**, 1 (1995).
[11] N. C. Tsamis and R. P. Woodard, Annals Phys., **253**, 1 (1997), arXiv:hep-ph/9602316.
[12] N. C. Tsamis and R. P. Woodard, Nucl. Phys., **B474**, 235 (1996), arXiv:hep-ph/9602315.
[13] N. C. Tsamis and R. P. Woodard, Nucl. Phys., **B724**, 295 (2005), arXiv:gr-qc/0505115.
[14] A. Higuchi and S. S. Kouris, Class. Quant. Grav., **18**, 2933 (2001), arXiv:gr-qc/0011062.
[15] A. Higuchi and S. S. Kouris, Class. Quant. Grav., **18**, 4317 (2001), arXiv:gr-qc/0107036.
[16] A. Higuchi and R. H. Weeks, Class. Quant. Grav., **20**, 3005 (2003), arXiv:gr-qc/0212031.
[17] A. M. Polyakov, Nucl. Phys., **B797**, 199 (2008), arXiv:0709.2899 [hep-th].

[18] G. Perez-Nadal, A. Roura, and E. Verdaguer, Class. Quant. Grav., **25**, 154013 (2008), arXiv:0806.2634 [gr-qc].
[19] M. Faizal and A. Higuchi, Phys. Rev., **D78**, 067502 (2008), arXiv:0806.3735 [gr-qc].
[20] E. T. Akhmedov and P. V. Buividovich, Phys. Rev., **D78**, 104005 (2008), arXiv:0808.4106 [hep-th].
[21] A. Higuchi, Class. Quant. Grav., **26**, 072001 (2009).
[22] A. Higuchi and Y. C. Lee, Classical and Quantum Gravity, **26**, 135019 (2009), arXiv:0903.3881 [gr-qc].
[23] E. T. Akhmedov, (2009), arXiv:0909.3722 [hep-th].
[24] A. M. Polyakov, Nucl. Phys., **B834**, 316 (2010), arXiv:0912.5503 [hep-th].
[25] C. P. Burgess, R. Holman, L. Leblond, and S. Shandera, Journal of Cosmology and Astroparticle Physics, **2010**, 017 (2010), arXiv:1005.3551 [hep-th].
[26] S. B. Giddings and M. S. Sloth, (2010), arXiv:1005.1056 [hep-th].
[27] D. Marolf and I. A. Morrison, In press. To appear in Phys. Rev. D. (2010), arXiv:1006.0035 [gr-qc].
[28] J. B. Hartle and S. W. Hawking, Phys. Rev., **D13**, 2188 (1976).
[29] G. Perez-Nadal, A. Roura, and E. Verdaguer, JCAP, **1005**, 036 (2010), arXiv:0911.4870 [gr-qc].
[30] O. Nachtmann, Osterr. Akad. Wiss., Math.-Naturw., Abt. II, **176**, 363 (1968).
[31] N. P. Myhrvold, Phys. Rev. D, **28**, 2439 (1983).
[32] J. Bros, H. Epstein, and U. Moschella, JCAP, **0802**, 003 (2008), arXiv:hep-th/0612184.
[33] D. Boyanovsky, R. Holman, and S. Prem Kumar, Phys.Rev., **D56**, 1958 (1997), arXiv:hep-ph/9606208 [hep-ph].
[34] S. Hollands and R. M. Wald, Commun. Math. Phys., **293**, 85 (2010), arXiv:0803.2003 [gr-qc].
[35] S. Hollands and R. M. Wald, Commun. Math. Phys., **231**, 309 (2002), arXiv:gr-qc/0111108.
[36] S. Hollands, (2010), arXiv:1010.5367 [gr-qc].
[37] N. D. Birrell and P. C. W. Davies, *Quantum Fields In Curved Space* (1982) cambridge, Uk: Univ. Pr. 340p.
[38] N. Y. Vilenken and A. U. Klimyk, *Representations of Lie Groups and Special Functions*, Vol. 1-3 (Dordrecht: Klower Acad. Publ., 1991).
[39] K. Goldstein and D. A. Lowe, Phys. Rev., **D69**, 023507 (2004), arXiv:hep-th/0308135.
[40] R. Bousso, A. Maloney, and A. Strominger, Phys. Rev., **D65**, 104039 (2002), arXiv:hep-th/0112218.
[41] J. de Boer, V. Jejjala, and D. Minic, Phys. Rev., **D71**, 044013 (2005), arXiv:hep-th/0406217.
[42] K. Goldstein and D. A. Lowe, Nucl. Phys., **B669**, 325 (2003), arXiv:hep-th/0302050.
[43] K. Goldstein, *de Sitter space, interacting quantum field theory and alpha vacua*, Ph.D. thesis, Brown University, Providence, Rhode Island (2001), uMI-31-74611.
[44] M. B. Einhorn and F. Larsen, Phys. Rev., **D67**, 024001 (2003), arXiv:hep-th/0209159.
[45] M. B. Einhorn and F. Larsen, Phys. Rev., **D68**, 064002 (2003), arXiv:hep-th/0305056.
[46] R. Brunetti, K. Fredenhagen, and S. Hollands, JHEP, **05**, 063 (2005), arXiv:hep-th/0503022.
[47] V. A. Smirnov, Springer Tracts Mod. Phys., **211**, 1 (2004).
[48] N. Bogoliubov and D. Shirkov, *Introduction to the theory of quantized fields* (Wiley New York, 1980).
[49] D. Marolf and I. A. Morrison, In preparation.
[50] A. Rajaraman, (2010), arXiv:1008.1271 [hep-th].
[51] D. Schlingemann, (1999), arXiv:hep-th/9912235.
[52] J. Glimm and A. M. Jaffe, *QUANTUM PHYSICS. A FUNCTIONAL INTEGRAL POINT OF VIEW* (1987) new York, Usa: Springer 535p.
[53] A. Higuchi, D. Marolf, and I. A. Morrison, In preparation (2010).
[54] A. Erdelyi, ed., *Higher transcendental functions*, Bateman Manuscript Project, Vol. 1 (McGraw-Hill, New York, 1953).